http://dx.doi.org/10.7567/JJAP.52.08JC08

Semipolar ($20\bar{2}1$) Single-Quantum-Well Red Light-Emitting Diodes with a Low Forward Voltage

Yoshinobu Kawaguchi[1,2], Chia-Yen Huang[1], Yuh-Renn Wu[3], Yuji Zhao[4],
Steven P. DenBaars[1,4], and Shuji Nakamura[1,4]

[1] *Department of Materials, University of California, Santa Barbara, CA 93106, U.S.A.*
[2] *Advanced Technology Research Laboratories, Sharp Corporation, Tenri, Nara 632-8567, Japan*
[3] *Institute of Photonics and Optoelectronics and Department of Electrical Engineering, National Taiwan University, Taipei 10617, Taiwan*
[4] *Department of Electrical and Computer Engineering, University of California, Santa Barbara, CA 93106, U.S.A.*

Received October 12, 2012; accepted March 24, 2013; published online June 20, 2013

We have demonstrated the InGaN/GaN single-quantum-well (SQW) red light-emitting diodes (LEDs) grown on the free-standing GaN ($20\bar{2}1$) substrate with a forward voltage as low as 2.8 V at 20 mA. A low p-GaN growth temperature is required to prevent the structure deterioration during the p-GaN growth. The reduction of the forward voltage was observed as the emission wavelength increased in the ($20\bar{2}1$) SQW LEDs, which is attributed to its reversed polarization-related electric field compared to the conventional *c*-plane LEDs.
© 2013 The Japan Society of Applied Physics

1. Introduction

InGaN alloys possess a wide range of bandgap from the infrared to the ultraviolet region. Blue and green InGaN light-emitting diodes (LEDs) are studied extensively and already are commercially available. On the other hand, not so many studies have been conducted regarding red InGaN LEDs[1–5] and they are not commercialized yet. The crystal growth of InGaN red LEDs is regarded as a challenge due to the difficulty in growing InGaN with high In composition.[6] The poor crystal quality impedes the commercialization of InGaN red LEDs. Additionally, the huge polarization-related field in the highly-strained InGaN quantum wells (QWs) also deteriorates the emission efficiency because of the quantum confinement Stark effect (QCSE) in conventional *c*-plane LEDs.[7,8]

The semipolar ($20\bar{2}1$) plane has drawn considerable attention since the realization of the high quality green laser diodes (LDs) on this plane.[9–12] The InGaN QWs with high In composition grown on the ($20\bar{2}1$) plane showed the good crystal quality in the green region.[9,13] The influence of the QCSE is also mitigated by the reduced polarization-related electric field.[14–16] In addition, a unique property was recently reported about the carrier transport in the ($20\bar{2}1$) plane.[17] The study showed that the single-quantum-well (SQW) structure was favorable for the ($20\bar{2}1$) LEDs in terms of both electroluminescence (EL) intensity and forward voltage due to the poor carrier transport in the multi-quantum-well (MQW) structure.

In this paper, we selected the ($20\bar{2}1$) SQW LEDs in order to study InGaN red LEDs because the ($20\bar{2}1$) plane is suitable for the longer wavelength region and the SQW structure is favorable for the ($20\bar{2}1$) LEDs as mentioned above. We investigated the effect of the p-GaN growth temperature on the emission wavelength because the growth temperature of the p-GaN was reported to be relevant to the dissociation of InGaN.[18–20] We obtained red LEDs with a low forward voltage by decreasing the p-GaN growth temperature. We also compared the wavelength dependence of the forward voltage between the ($20\bar{2}1$) and ($20\bar{2}\bar{1}$) SQW LEDs to consider the origin of the low forward voltage of the ($20\bar{2}1$) SQW red LEDs.

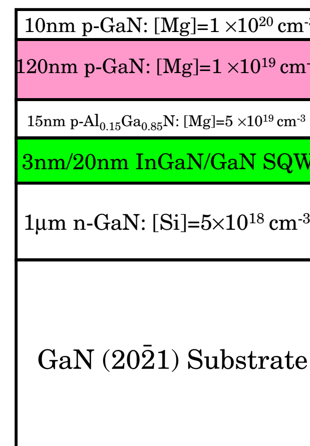

Fig. 1. (Color online) The schematic illustration of the epitaxial structure.

2. Sample Structure

The ($20\bar{2}1$) SQW LEDs with the p-GaN layer grown at different temperatures (810 °C, 910 °C, 1010 °C) were fabricated by metalorganic chemical vapor deposition (MOCVD) on the free-standing GaN ($20\bar{2}1$) substrate manufactured by Mitsubishi Chemical Corporation.[21] The epitaxial structure consisted of a 1 μm Si-doped n-GaN ($[Si] = 5 \times 10^{18}$ cm^{-3}) layer and an undoped active region with a 3 nm InGaN SQW sandwiched by 20 nm GaN barriers. A 15 nm Mg-doped p-$Al_{0.15}Ga_{0.85}N$ ($[Mg] = 5 \times 10^{19}$ cm^{-3}) electron-blocking layer (EBL) was deposited and followed by a 120 nm Mg-doped p-GaN ($[Mg] = 1 \times 10^{19}$ cm^{-3}) layer with a 10 nm heavily Mg-doped p-GaN contact layer ($[Mg] = 1 \times 10^{20}$ cm^{-3}) on top, as illustrated in Fig. 1. The emission wavelength of LEDs was manipulated by the growth temperature of the QW.

3. Results and Discussion

Figure 2(a) shows the relationship between the EL wavelength under 20 A/cm^2 and the growth temperature of the QW. The injection area was a circle with a diameter of 340 μm. The p-GaN growth temperatures did not have a

 © 2013 The Japan Society of Applied Physics

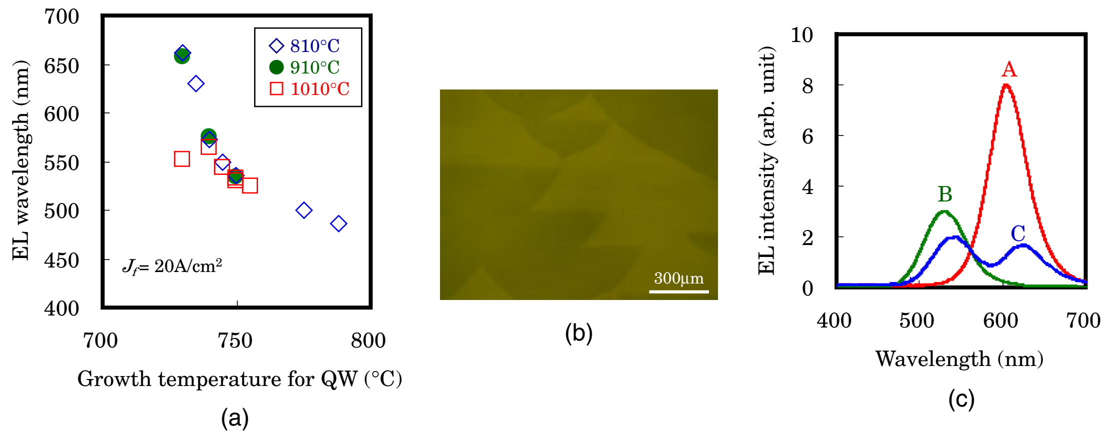

Fig. 2. (Color online) (a) The relationship between the EL wavelength and the growth temperature for the QW with the different growth temperatures for the p-GaN layer (810 °C, 910 °C, 1010 °C). (b) The fluorescence microscope image of the sample surface grown at 735 °C for the QW with p-GaN grown at 1010 °C. (c) The EL spectra measured at the different positions (A: the outside of the triangular-shaped areas, B: the inside of the triangular-shaped areas, and C: the position containing both the inside and the outside of the triangular-shaped areas).

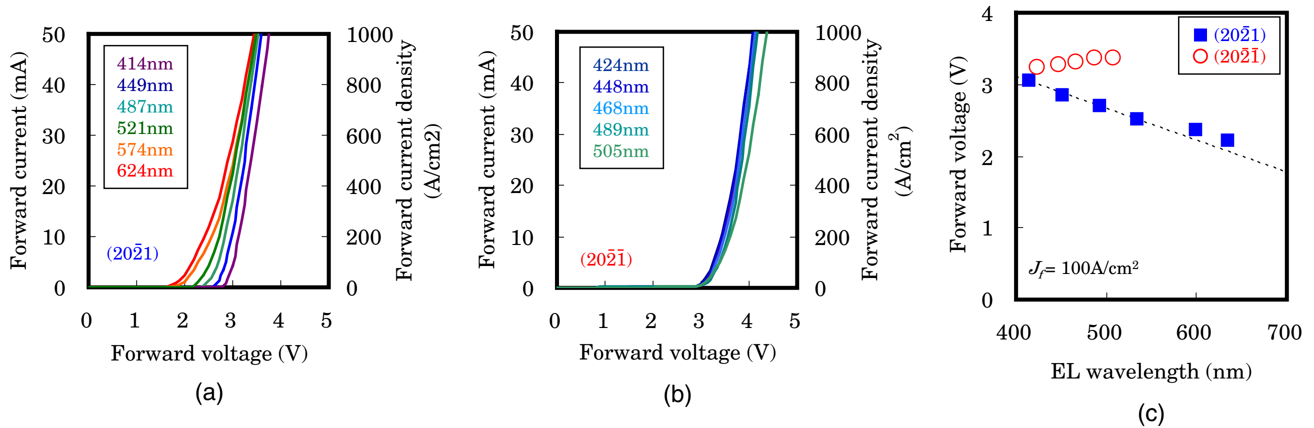

Fig. 3. (Color online) The current–voltage characteristics of the (a) (20$\bar{2}$1) and (b) (20$\bar{2}\bar{1}$) SQW LEDs with the various emission wavelengths. The mission wavelengths shown in the graphs are the values measured at 20 mA (400 A/cm^2). (c) The wavelength dependence of the forward voltage at 5 mA (100 A/cm^2) of the (20$\bar{2}$1) and (20$\bar{2}\bar{1}$) SQW LEDs. The broken line shows the photon energy of the emission wavelength.

strong impact on the EL wavelength when the growth temperature of the QW was higher than 740 °C. The EL wavelength became longer by further decreasing the QW growth temperature when the p-GaN growth temperature was less than 910 °C. As a result, the red EL emission was obtained within the range of 730–735 °C for the QW growth temperature. However, under the condition of 1010 °C for the p-GaN growth temperature, the EL wavelength became even shorter when the QW growth temperature was reduced from 740 to 730 °C, which implies that high p-GaN growth temperature could be a limiting factor for increasing the EL wavelength. In order to investigate this unusual wavelength shift, the LED with the QW grown at 735 °C and the p-GaN grown at 1010 °C was examined in detail. Figure 2(b) is a fluorescence microscope image of this LED. Triangular-shaped areas with dimmer emission were observed. Figure 2(c) is EL spectra of this LED acquired at the different positions. Three types of spectra were observed depending on the positions. The longer wavelength emission (A) and the shorter one (B) were observed at the outside of the triangular-shaped areas and the inside of those areas, respectively. The emission at the position containing both areas showed two peaks (C) corresponding to the wavelength of A and B. These results indicate that In composition was less inside the triangular-shaped areas and that the spread of these areas to the entire surface caused the unusual shift toward the shorter wavelength as seen in the LED with the QW grown at 730 °C. However, those triangular-shaped areas were not observed in the LEDs with the p-GaN grown at 810 and 910 °C even when their QWs were grown at 730 °C. Therefore, the triangular-shaped areas were highly likely to be formed during the high temperature p-GaN growth. The detailed defect structures inside the triangle-shaped areas are still under investigation. But we can still draw the conclusion that a low p-GaN growth temperature is necessary in order to achieve longer wavelength emissions.

Figure 3(a) is current–voltage characteristics of the (20$\bar{2}$1) SQW LEDs with the various emission wavelengths. The injection area was a circle with a diameter of 80 μm. In addition to the (20$\bar{2}$1) SQW LEDs, the (20$\bar{2}\bar{1}$) SQW LEDs with the same structure were also investigated for comparison as shown in Fig. 3(b). The turn-on voltages of the

 © 2013 The Japan Society of Applied Physics

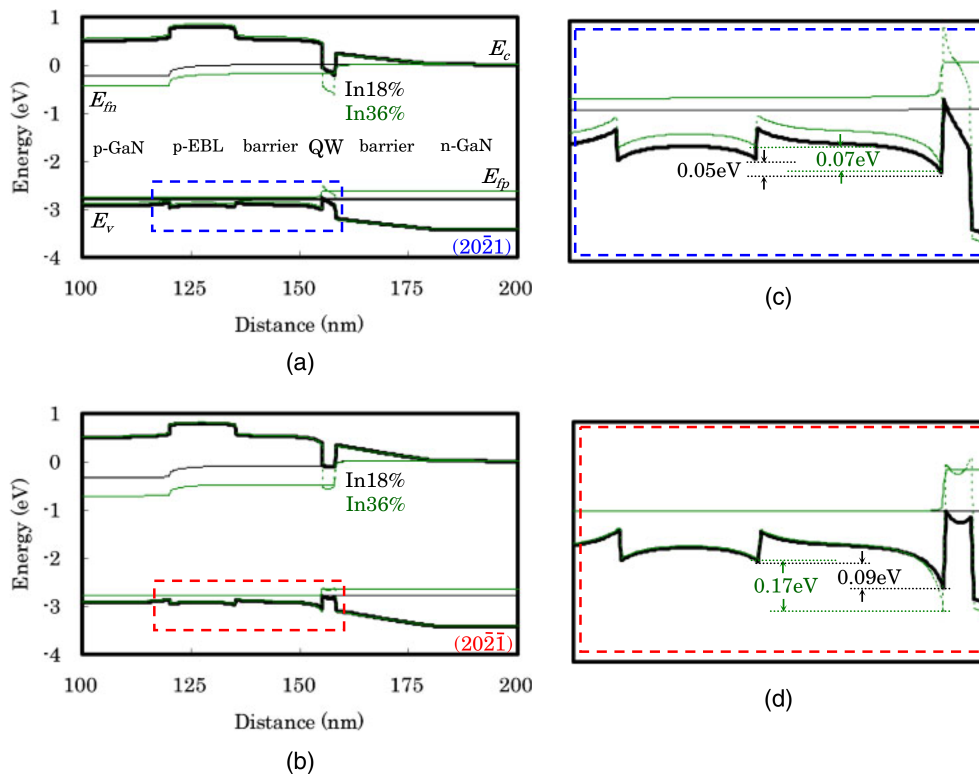

Fig. 4. (Color online) The calculated band diagrams for the (a) (20$\bar{2}$1) and (b) (20$\bar{2}\bar{1}$) SQW LEDs under the same forward bias (2.8 V). The magnification of the band diagrams at the highlighted area of the (c) (20$\bar{2}$1) and (d) (20$\bar{2}\bar{1}$) planes.

(20$\bar{2}$1) SQW LEDs were significantly reduced as the emission wavelengths increased whereas those of the (20$\bar{2}\bar{1}$) SQW LEDs were not significantly influenced by the emission wavelength. The forward voltage of the (20$\bar{2}$1) SQW LED with a 624 nm emission wavelength (estimated In composition: 36%) at 20 mA (400 A/cm^2) was as low as 2.8 V. The author would like to note that the high series resistance in the longer wavelength LEDs might be caused by the deterioration of the crystal quality in the active region or the p-GaN. With further improvement in crystal quality, the forward voltage is expected to become even lower.

The dependence of the forward voltage at 5 mA (100 A/cm^2) on the emission wavelength was plotted as shown in Fig. 3(c). The forward voltage of the (20$\bar{2}$1) SQW LEDs decreased as the emission wavelengths increased. The theoretical minimum voltage of LEDs is limited by the photon energy according to the law of conservation of energy. However, the additional forward voltage can be built by the polarization-related electric fields or parasitic sheet resistances.[22] Since the voltage was in close agreement with its emission photon energy, which is shown as a broken line in Fig. 3(c), we suggest that the (20$\bar{2}$1) SQW LEDs do not have significant additional injection barriers compared to ideal diodes. On the other hand, the forward voltage of the (20$\bar{2}\bar{1}$) SQW LEDs slightly increased as the emission wavelengths increased. This implies that the additional injection barriers are accompanied by the increase of the In composition for the (20$\bar{2}\bar{1}$) SQW LEDs.

Band diagram simulations were conducted in order to investigate the origin of the different behaviors between the (20$\bar{2}$1) and (20$\bar{2}\bar{1}$) SQW LEDs. A self-consistent 1D Poisson, drift-diffusion and Schrödinger numerical solver[23] was applied to calculate the band structure. The calculated band diagrams for the (20$\bar{2}$1) and (20$\bar{2}\bar{1}$) SQW LEDs under the same forward bias (2.8 V) are shown in Figs. 4(a) and 4(b), respectively. Two different values of the In composition (18 and 36%) were calculated to examine the influence of the In composition. The barrier heights for holes and electrons to the QW are lower in the (20$\bar{2}$1) SQW LEDs than in the (20$\bar{2}\bar{1}$) SQW LEDs as seen in Figs. 4(a) and 4(b). This is because in the (20$\bar{2}$1) plane the antiparallel polarization-related field in the barrier to the built-in p–n junction electric field diminishes the barrier height at the interface between the barrier and the QW.[17,24,25] This favorable direction of the polarization-related field for carrier injection into the QW is the origin of the low forward voltage in the (20$\bar{2}$1) SQW LEDs. Figures 4(c) and 4(d) are the magnification of the band diagrams at the highlighted areas of Figs. 4(a) and 4(b), respectively. Figure 4(c) shows that the barrier height from EBL to QW/barrier interface is not sensitive to the In composition of the QWs. Therefore, the forward voltage is dominated by the bandgap of the QW as seen experimentally in Fig. 3(c). On the contrary, in the (20$\bar{2}\bar{1}$) SQW LEDs the injection barrier heights for holes and electrons to the QW are enhanced by the polarization-related electric field due to its reversed polarity compared to the (20$\bar{2}$1) SQW LEDs.[17,26] Moreover, the injection barrier is further enhanced as the In composition increases as seen in Fig. 4(d) because the higher In composition causes the larger polarization-related electric field. This suggests that the enhanced injection barrier heights compensate or outweigh the effect of the narrower bandgap in the (20$\bar{2}\bar{1}$) SQW LEDs, which results in the different trend from the (20$\bar{2}$1) SQW LEDs as seen experimentally in Fig. 3(c).

© 2013 The Japan Society of Applied Physics

4. Conclusions

In summary, the $(20\bar{2}1)$ red SQW LEDs with a low forward voltage was demonstrated. In order to obtain the red emission, the p-GaN growth temperature has to be reduced compared to that in the conventional blue LEDs because excessively high p-GaN growth temperature caused triangular areas with a reduced emission wavelength. The reduction of the forward voltage in the longer wavelength was caused by the combination of the low injection barriers in the $(20\bar{2}1)$ SQW LEDs and the narrower bandgap of the QW.

Acknowledgements

The authors would like to thank Mitsubishi Chemical Corporation for the supply of bulk GaN substrates. The authors acknowledge the Solid State Lighting and Energy Center (SSLEC) at UCSB and the support of the NSF MRSEC program (DMR 1121053) for MRL characterization facilities. A portion of this work was performed in the UCSB nanofabrication facility, part of the National Science Foundation (NSF)-funded National Nanotechnology Infrastructure Network (NNIN). This work is partially supported by National Science Council in Taiwan under grant NSC-99-2221-E-002-058-MY3.

1) T. Mukai, M. Yamada, and S. Nakamura: Jpn. J. Appl. Phys. **38** (1999) 3976.
2) Y. Yamashita, H. Tamura, N. Horio, H. Sato, K. Taniguchi, T. Chinone, S. Omori, and C. Funaoka: Jpn. J. Appl. Phys. **42** (2003) 4197.
3) H. S. Chen, C. F. Lu, D. M. Yeh, C. F. Huang, J. J. Huang, and C. C. Yang: IEEE Photonics Technol. Lett. **18** (2006) 2269.
4) C. Y. Huang, Q. Yan, Y. Zhao, K. Fujito, D. Feezell, C. G. V. de Walle, J. S. Speck, S. P. DenBaars, and S. Nakamura: Appl. Phys. Lett. **99** (2011) 141114.
5) K. Ohkawa, T. Watanabe, M. Sakamoto, A. Hirako, and M. Deura: J. Cryst. Growth **343** (2012) 13.
6) I.-h. Ho and G. B. Stringfellow: Appl. Phys. Lett. **69** (1996) 2701.
7) S. Chichibu, T. Azuhata, T. Sota, and S. Nakamura: Appl. Phys. Lett. **69** (1996) 4188.
8) T. Takeuchi, S. Sota, M. Katsuragawa, M. Komori, H. Takeuchi, H. Amano, and I. Akasaki: Jpn. J. Appl. Phys. **36** (1997) L382.
9) Y. Enya, Y. Yoshizumi, T. Kyono, K. Akita, M. Ueno, M. Adachi, T. Sumitomo, S. Tokuyama, T. Ikegami, K. Katayama, and T. Nakamura: Appl. Phys. Express **2** (2009) 082101.
10) Y. Yoshizumi, M. Adachi, Y. Enya, T. Kyono, S. Tokuyama, T. Sumitomo, K. Akita, T. Ikegami, M. Ueno, K. Katayama, and T. Nakamura: Appl. Phys. Express **2** (2009) 092101.
11) M. Adachi, Y. Yoshizumi, Y. Enya, T. Kyono, T. Sumitomo, S. Tokuyama, S. Takagi, K. Sumiyoshi, N. Saga, T. Ikegami, M. Ueno, K. Katayama, and T. Nakamura: Appl. Phys. Express **3** (2010) 121001.
12) Y. D. Lin, Y. Yamamoto, C. Y. Huang, C. L. Hsiung, F. Wu, K. Fujito, H. Ohta, J. S. Speck, S. P. DenBaars, and S. Nakamura: Appl. Phys. Express **3** (2010) 082001.
13) M. Funato, A. Kaneta, Y. Kawakami, Y. Enya, K. Nishizuka, M. Ueno, and T. Nakamura: Appl. Phys. Express **3** (2010) 021002.
14) T. Takeuchi, H. Amano, and I. Akasaki: Jpn. J. Appl. Phys. **39** (2000) 413.
15) S. H. Park and S. L. Chuang: Phys. Rev. B **59** (1999) 4725.
16) A. E. Romanov, T. J. Baker, S. Nakamura, and J. S. Speck: J. Appl. Phys. **100** (2006) 023522.
17) Y. Kawaguchi, C. Y. Huang, Y. R. Wu, Q. Yan, C. C. Pan, Y. Zhao, S. Tanaka, K. Fujito, D. Feezell, C. G. V. de Walle, S. P. DenBaars, and S. Nakamura: Appl. Phys. Lett. **100** (2012) 231110.
18) P. T. Barletta, E. A. Berkman, B. F. Moody, N. A. El-Masry, A. M. Emara, M. J. Reed, and S. M. Bedair: Appl. Phys. Lett. **90** (2007) 151109.
19) H. K. Cho, T. E. Park, D. C. Kim, J. E. Shin, and J. S. Lee: Phys. Status Solidi B **241** (2004) 2816.
20) Y. L. Hu, R. M. Farrell, C. J. Neufeld, M. Iza, S. C. Cruz, N. Pfaff, D. Simeonov, S. Keller, S. Nakamura, S. P. DenBaars, U. K. Mishra, and J. S. Speck: Appl. Phys. Lett. **100** (2012) 161101.
21) K. Fujito, K. Kiyomi, T. Mochizuki, H. Oota, H. Namita, S. Nagao, and I. Fujimura: Phys. Status Solidi A **205** (2008) 1056.
22) E. F. Schubert: *Light-Emitting Diodes* (Cambridge University Press, Cambridge, U.K., 2006) 2nd ed., p. 83.
23) C. K. Li and Y. R. Wu: IEEE Trans. Electron Devices **59** (2012) 400.
24) F. Akyol, D. N. Nath, S. Krishnamoorthy, P. S. Park, and S. Rajan: Appl. Phys. Lett. **100** (2012) 111118.
25) A. Konar, A. Verma, T. Fang, P. Zhao, R. Jana, and D. Jena: Semicond. Sci. Technol. **27** (2012) 024018.
26) D. F. Feezell, J. S. Speck, S. P. DenBaars, and S. Nakamura: J. Disp. Technol. **9** (2013) 190.

© 2013 The Japan Society of Applied Physics